
Low Rank Saddle Free Newton: Algorithm and Analysis

Thomas O’Leary-Roseberry¹ Nick Alger¹ Omar Ghattas¹

Abstract

Many tasks in engineering fields and machine learning involve minimizing a high dimensional non-convex function. The existence of saddle points poses a central challenge in practice. The Saddle Free Newton (SFN) algorithm can rapidly escape high dimensional saddle points by using the absolute value of the Hessian of the empirical risk function. In SFN, a Lanczos type procedure is used to approximate the absolute value of the Hessian. Motivated by recent empirical works that note neural network training Hessians are typically low rank, we propose using approximation via scalable randomized low rank methods. Such factorizations can be efficiently inverted via Sherman Morrison Woodbury formula. We derive bounds for convergence rates in expectation for a stochastic version of the algorithm, which quantify errors incurred in subsampling as well as in approximating the Hessian via low rank factorization. We test the method on standard neural network training benchmark problems: MNIST and CIFAR10. Numerical results demonstrate that in addition to avoiding saddle points, the method can converge faster than first order methods, and the Hessian can be subsampled significantly relative to the gradient and retain superior performance for the method.

1. Introduction

We consider the stochastic optimization problem

$$\min_{w \in \mathbb{R}^d} F(w) = \int \ell(w; x, y) d\nu(x, y) \quad (1)$$

where ℓ is a smooth loss function, $w \in \mathbb{R}^d$ is the vector of optimization variables and the data pairs (x, y) are distributed with joint probability distribution $\nu(x, y)$. $F : \mathbb{R}^d \rightarrow \mathbb{R}$ is referred to as the expected risk function. This problem

arises in machine learning, where the goal is to reconstruct a mapping $x \mapsto y$ with a deep neural network or other model parameterized by w . In practice ν is not known, and instead one only has access to samples $x_i, y_i \sim \nu$. Given a sample dataset $X = \{(x_i, y_i) \sim \nu\}_{i=1}^{N_X}$, a Monte Carlo approximation of the expected risk minimization problem, Equation 1, leads to the empirical risk minimization problem:

$$\min_{w \in \mathbb{R}^d} F_X(w) = \frac{1}{N_X} \sum_{i=1}^{N_X} \ell(w; x_i, y_i). \quad (2)$$

Optimization problem (2) serves as a surrogate for (1).

In many settings such as deep learning, problems (1) and (2) are nonconvex. Nonconvexity makes it computationally intractable (NP-hard) to find global minima (Bertsekas, 1997; Murty & Kabadi, 1987). It is also generally not the case that the global minimizer of (2) is the global minimizer of (1). Thus iterative (gradient-based) methods of the form

$$w_{k+1} = w_k + \alpha_k p_k \quad (3)$$

are typically used to explore the nonconvex energy landscape for (2), searching for local minima that generalize well to unseen data. Here p_k is a search direction, and α_k is a step length parameter.

Nonconvex energy landscapes typically contain many strict saddle points (stationary points with at least one direction of negative curvature). Much work has been dedicated to understanding how first order methods perform in the vicinity of strict saddle points (Ge et al., 2015; Jin et al., 2017; Lee et al., 2017; 2016). Saddle points slow the local convergence of first order methods (methods in which p_k is constructed using only gradient information). These methods typically escape saddle points asymptotically. Newton’s method without modification converges locally to strict saddle points, since gradient components initially oriented away from the saddle are reoriented towards the saddle point due to the associated negative eigenvalue of the Hessian.

Newton methods can be adapted to escape saddle points by enforcing positive definiteness of the Hessian matrix,

$$H := \nabla^2 F_X.$$

One approach that facilitates fast escape from saddle points involves replacing the Hessian with the absolute value of

¹Oden Institute for Computational Engineering and Sciences, The University of Texas at Austin, Austin, TX. Correspondence to: Thomas O’Leary-Roseberry <tom@oden.utexas.edu>.

the Hessian, $|H|$ (Gill et al., 1981). By the absolute value of the Hessian, we mean the matrix that is the same as the Hessian, except the negative eigenvalues are flipped to be positive. Specifically, let the spectral decomposition of the Hessian be given as follows:

$$H = U\Lambda U^T = \sum_{i=1}^d \lambda_i u_i u_i^T, \quad (4)$$

where the eigenvalues λ_i are sorted such that $|\lambda_i| \geq |\lambda_j|$ for all $i > j$, and $u_i \in \mathbb{R}^d$ are the associated eigenvectors. The absolute value of the Hessian thus is

$$|H| = \sum_{i=1}^d |\lambda_i| u_i u_i^T.$$

Then $|H|$ is used in place of H within the Newton system. Moreover, rank deficiency of the Hessian is often addressed via ℓ^2 regularization or Levenberg-Marquardt damping. With these modifications the Newton system becomes

$$(|H| + \gamma I) p_k = -g_k, \quad (5)$$

where γ is a regularization or damping parameter, and g_k is the gradient. By using $|H|$ rather than H , iterates w_k escape saddle points quickly, because flipping the sign of the eigenvalue causes saddle points to repel the iterates.

Classically, $|H|$ is computed by forming the dense Hessian matrix, which requires $O(N_X d^2)$ work, then performing a spectral decomposition of this matrix, which requires $O(d^3)$ work. In deep learning d is large, so formation and factorization of the Hessian is not computationally tractable. The Saddle Free Newton (SFN) algorithm (Dauphin et al., 2014) addresses this difficulty by using the Lanczos procedure to form an approximation of $|H|$. Computing the Lanczos approximation of order r does not require forming or factorizing the Hessian matrix; instead only the application of the Hessian to r vectors is required.

Typically it is too expensive to use all N_X samples at each iteration. It is standard practice, therefore, to subsample the gradient and Hessian at each iteration (use a small subset of the data pairs to form the gradient and Hessian). Recently it has been shown that Newton-type algorithms converge rapidly even when the Hessian is subsampled more than the gradient, because the variance of the Hessian is typically smaller than that of the gradient (Erdogdu & Montanari, 2015; Roosta-Khorasani & Mahoney, 2016a;b; Xu et al., 2016). In the remainder of this paper, all Hessians and gradients are subsampled. We denote the gradient batch size at iteration k by N_{X_k} and the Hessian batch size by N_{S_k} .

2. Low Rank Saddle Free Newton

Recent empirical studies of their spectra show that neural network training Hessians are typically numerically low

rank, and when away from local minima often have at least one large magnitude negative eigenvalue (Alain et al., 2019; Ghorbani et al., 2019; Sagun et al., 2016). In this work we therefore propose forming a low rank approximation of the Hessian,

$$H_r = [\nabla^2 F]_r = U_r \Lambda_r U_r^T = \sum_{i=1}^r \lambda_i u_i u_i^T. \quad (6)$$

using the double pass randomized eigenvalue decomposition in Algorithm 5.3 of (Halko et al., 2011), instead of the Lanczos procedure. The rank r can be chosen such that the trailing eigenvalues are smaller than some tolerance $|\lambda_j| < \epsilon_H$ for all $j > r$. Like Lanczos, this algorithm avoids forming the Hessian, and instead employs only r products of the Hessian with random vectors.¹ We use this low rank approximation, in combination with the Sherman-Morrison-Woodbury formula, to solve the modified Newton system (5) as follows:

$$p_k = -\left[\frac{1}{\gamma} I_d - \frac{1}{\gamma^2} U_r \left(|\Lambda_r|^{-1} + \frac{1}{\gamma} I_r \right)^{-1} U_r^T \right] g_k. \quad (7)$$

The low rank saddle free Newton (LRSFN) method is summarized in Algorithm 1.

Algorithm 1 Low Rank Saddle Free Newton

Given w_0
while Not converged **do**
 Compute the randomized approximation
 $U_r^{(k)} \Lambda_r U_r^{(k)T} \approx H_r$
 Compute p_k using Equation (7)
 α_k given or computed via line search
 $w_{k+1} = w_k + \alpha_k p_k$
end while

3. Low Rank vs. Krylov

On one hand, the Eckart-Young Theorem states that the low rank approximation (6) is optimal in the spectral and Frobenius norms. On the other hand, Krylov approximations such as Lanczos are optimal in the sense of certain polynomial approximations; for more details see (Saad, 2003). So which one is better here? We claim that randomized low rank approximation is better in this setting. It (a) leads to solutions that generalize better when the Hessian is subsampled, (b) is better at escaping saddle points, and (c) is better suited for modern parallel computer architectures.

(a) The objective function is most sensitive to perturbations of w in directions corresponding to eigenvalues of large magnitude, since the energy landscape has large curvature

¹Actually, the Hessian is typically oversampled, so that $r + p$ random vectors are used, where p is typically much smaller than r .

in these directions. These directions typically persist when different sets of subsamples are used to approximate the Hessian. Directions corresponding to eigenvalues of small magnitude are less important since the objective function is less sensitive to perturbations in these directions. These directions tend to fluctuate when different sets of subsamples are used to approximate the Hessian. Since Krylov methods approximate the whole spectrum, they waste computational effort attempting to approximate eigenvalues of small magnitude that vary depending on the random subsamples used. Low rank approximation only approximates the large eigenvalues, and therefore leads to solutions that generalize better.

(b) Krylov subspace approximations are heavily dependent on the initial vector for the subspace. In Newton-Krylov methods such as SFN, the gradient is the initial vector. However in the vicinity of a saddle point the gradient may have small components in eigenvector directions corresponding to eigenvalues that are negative but large in magnitude. Randomized low rank methods are better than Krylov methods at capturing these large magnitude directions when the gradient is small in these directions. Hence LRSFN pushes iterates away from saddle points more strongly than Krylov-based Saddle Free Newton.

(c) Krylov methods are inherently serial, while the matrix-vector products required by randomized low rank methods are independent and therefore easily parallelized.

For a general discussion of randomized methods and Krylov methods, see (Martinsson & Tropp, 2020).

4. Semi-stochastic convergence rate

In this section we prove asymptotic bounds for convergence rates of LRSFN, in expectation with respect to the training data used. These convergence rates quantify errors due to sampling, and errors due to the randomized procedure for performing the low-rank approximation of the Hessian. We present an expected bound for the convergence rates of the semi-stochastic version of the randomized LRSFN algorithm. In this case only the Hessian is subsampled, so there is no associated sampling error for the gradient. We denote by \mathbb{E}_ν the expectation with respect to ν , we denote by \mathbb{E}_k the conditional expectation at iteration k taken over all Hessian batch sizes of size N_{S_k} , and we denote by \mathbb{E}_ρ the expectation taken with respect to the Gaussian random matrices used in the randomized low rank approximation.

Assumption 1 (Bounded variance of Hessian components). *There exists $\sigma > 0$ such that*

$$\|\mathbb{E}_\nu[(\nabla^2 F_i(w) - \nabla^2 F(w))^2]\| \leq \sigma^2. \quad (8)$$

for all $w \in \mathbb{R}^d$.

Lemma 1. *If Assumption 1 holds, then*

$$\begin{aligned} & \mathbb{E}_k \left[\mathbb{E}_\rho [\| (H_r^{(k)} + \gamma I)(w_k) - \nabla^2 F(w_k) \|] \right] \\ & \leq \left(C |\overline{\lambda_{r+1}^{(k)}}| + \gamma + \frac{\sigma}{\sqrt{N_{S_k}}} \right) \end{aligned} \quad (9)$$

We have $C = 1$ in the case that the low rank approximation is exact, and $C = \left(1 + 4 \frac{\sqrt{d(r+p)}}{p-1} \right)$ when randomized low rank approximation is used with oversampling parameter p . Here, we use the shorthand $\mathbb{E}_k[\lambda_r^{(k)}] = \overline{\lambda_r^{(k)}}$.

Proof. When the randomized low rank decomposition is used, we have

$$\begin{aligned} & \mathbb{E}_k \left[\mathbb{E}_\rho [\| (H_r^{(k)} + \gamma I)(w_k) - \nabla^2 F(w_k) \|] \right] \\ & \leq \mathbb{E}_k \left[\mathbb{E}_\rho [\| (H_r^{(k)} + \gamma I)(w_k) - \nabla^2 F_{S_k}(w_k) \|] \right] \\ & \quad + \mathbb{E}_k [\| \nabla^2 F_{S_k}(w_k) - \nabla^2 F(w_k) \|]. \end{aligned} \quad (10)$$

We may bound the first term in (10) as follows:

$$\begin{aligned} & \mathbb{E}_k \left[\mathbb{E}_\rho [\| (H_r^{(k)} + \gamma I)(w_k) - \nabla^2 F_{S_k}(w_k) \|] \right] \\ & \leq \mathbb{E}_k \left[\left(1 + 4 \frac{\sqrt{d(r+p)}}{p-1} \right) |\lambda_{r+1}^{(k)}| + \gamma \right] \\ & = \left(1 + 4 \frac{\sqrt{d(r+p)}}{p-1} \right) \overline{|\lambda_{r+1}^{(k)}|} + \gamma \end{aligned} \quad (11)$$

The inequality in (11) comes from Equation 1.8 in (Halko et al., 2011). The second term in (10) is bounded by $\frac{\sigma}{\sqrt{N_{S_k}}}$ due to the bounded variance of Hessian components via Lemma 2.3 in (Bollapragada et al., 2018). \square

Theorem 1 (Expected convergence rate for semi-stochastic randomized low rank Newton). *Let w_k be in the basin of attraction of a local minimum w^* , and suppose that $\alpha_k = 1$, $\gamma > 0$ is chosen such that the Tikhonov regularization parameter γ satisfies $\gamma \neq \lambda_i$ for all λ_i , the Hessian is Lipschitz continuous with Lipschitz constant $M > 0$, and Assumption 1 holds. The iterates of the semi-stochastic randomized low rank Newton method satisfy the following bound:*

$$\mathbb{E}_{k,\rho} [\|w_{k+1} - w^*\|] \leq c_1 \|w_k - w^*\| + c_2 \|w_k - w^*\|^2 \quad (12)$$

where

$$\begin{aligned} c_1 = \frac{1}{|\lambda_* + \gamma|} & \left[\left(1 + 4 \frac{\sqrt{d(r+p)}}{p-1} \right) \overline{|\lambda_{r+1}^{(k)}|} \right. \\ & \left. + \gamma + \frac{\sigma}{\sqrt{N_{S_k}}} \right] \end{aligned} \quad (13)$$

$$c_2 = \frac{M}{2|\lambda_* + \gamma|} \quad (14)$$

and λ_* is the eigenvalue of $\nabla^2 F$ closest to $-\gamma$.

Proof. By a derivation in Lemma 2.2 in (Bollapragada et al., 2018) we have the following bound:

$$\|\nabla^2 F(w_k)(w_k - w^*) - \nabla F(w_k)\|^2 \leq \frac{M}{2} \|w_k - w^*\|^2. \quad (15)$$

This bound and the bound in Lemma 1, and the triangle inequality yield the following desired bound:

$$\begin{aligned} & \mathbb{E}_{k,\rho}[\|w_{k+1} - w^*\|] \\ &= \mathbb{E}_{k,\rho}[\|w_k - w^* - [H_r^{(k)} + \gamma I]^{-1}(w_k) \nabla F(w_k)\|] \\ &\leq \frac{1}{|\lambda_* + \gamma|} \mathbb{E}_{k,\rho}[\|([H_r^{(k)} + \gamma I](w_k) - \nabla^2 F(w_k))(w_k - w^*) \\ &\quad + \nabla^2 F(w_k)(w_k - w^*) - \nabla F(w_k)\|] \\ &\leq \frac{1}{|\lambda_* + \gamma|} \mathbb{E}_k[\|([H_r^{(k)} + \gamma I](w_k) - \nabla^2 F(w_k))(w_k - w^*)\|] \\ &\quad + \frac{1}{|\lambda_* + \gamma|} \|\nabla^2 F(w_k)(w_k - w^*) - \nabla F(w_k)\| \\ &\leq \frac{1}{|\lambda_* + \gamma|} \left(C |\overline{\lambda_{r+1}^{(k)}}| + \gamma + \frac{\sigma}{\sqrt{N_{S_k}}} \right) \|w_k - w^*\| \\ &\quad + \frac{M}{2|\lambda_* + \gamma|} \|w_k - w^*\|^2 \end{aligned}$$

□

When the error in the Hessian approximation approaches zero, one recovers the classic quadratic convergence bound of Newton’s method. Fast super-linear convergence can be observed when the low rank approximation is accurate ($|\lambda_{r+1}| \ll 1$), and the Hessian sampling error is small (small variance of Hessian components σ , or large Hessian batch size N_{S_k}). For the SFN method of Dauphin, a similar bound can be proven that will have the Krylov error in the linear error constant c_1 in place of the error stemming from the randomized approximation of the Hessian. For the fully stochastic case, an additional constant error term is incurred from the gradient sampling error. See (O’Leary-Roseberry et al., 2019) for more detailed convergence rates.

5. Numerical Experiments

We demonstrate the effectiveness of the LRSFN algorithm on the standard neural network benchmark problems MNIST (LeCun & Cortes, 2010) and CIFAR10 (Krizhevsky et al., 2010). We compare against standard first order methods as well as the Lanczos based SFN algorithm. Our LRSFN method outperforms these other methods.

Our focus is on comparing how the optimization methods perform for fixed neural network training problems, in a fixed number of neural network sweeps (we define a *sweep* as a forward or adjoint evaluation of the network). Finding optimal architectures for a given input-output representation is outside of the scope of this work. We compare the

performance of the LRSFN against an existing implementation of the SFN algorithm (Fernandes, 2019), as well as Adam and gradient descent (GD). In our implementation of LRSFN we implement different batching for the Hessian and gradient. In the SFN code of (Fernandes, 2019) this is not implemented, so we are constrained to use the same data for the gradient and Hessian in this method. We make some direct comparisons between the methods, where both use the same gradient and Hessian data. In general we compare all methods based on the number of neural network sweeps, as this is the primary computational cost in neural network training. For both MNIST and CIFAR10 we take 50,000 training data samples, from which batches used in training are sampled. We set aside 10,000 testing data samples in order to compute generalization (testing) errors. For all training problems we take $\gamma = 0.1$ and $r = 20$; r is both the rank of the low rank approximation and the Krylov dimension.

5.1. Dense classification (MNIST)

For the MNIST classification problem, we compare LRSFN against SFN, Adam, and GD. For GD and LRSFN we use line search (LS) to select α_k at each iteration. For Adam we test different step lengths $\alpha_k = 0.01, 0.001$ (larger step lengths had highly oscillatory behavior). The loss function for the training problem is the cross-entropy function. For GD and LRSFN we use gradient batch size $N_{X_k} = 10,000$, and for LRSFN we use Hessian batch size $N_{S_k} = 1000$. For Adam and SFN we use $N_{X_k} = 1000$ for the gradient, and as noted before, for SFN $N_{X_k} = N_{S_k}$. We use small data for SFN so that it doesn’t run out of neural network sweeps after just a few iterations. We have one hidden layer with 100 units; the size of the configuration space is $d = 79,510$.

The methods are judged based on how well the trained neural network classifies unseen data. Figures 1, 2, and 3 show that both SFN and LRSFN outperformed the first order methods and were less prone to overfitting. It is clear from the training and testing error plots that the first order methods overfit. Both of the second order methods generalized better to unseen data, and LRSFN had the highest classification accuracy.

5.2. Convolutional autoencoders

In our second set of numerical experiments, we train convolutional autoencoders on the MNIST and CIFAR10 data sets. For the convolutional autoencoder training problem a least squares loss function is used to measure the error in reconstructing input images with a four layer autoencoder network. For the MNIST problem $d = 517$, for the CIFAR10 problem $d = 1543$; the goal of the autoencoder is to compress information, the training problem is therefore overdetermined.

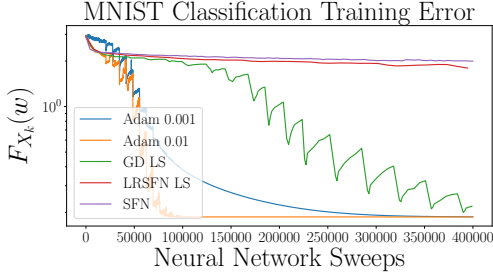


Figure 1. MNIST classification training error

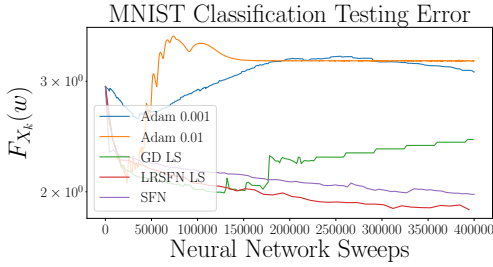


Figure 2. MNIST classification testing error

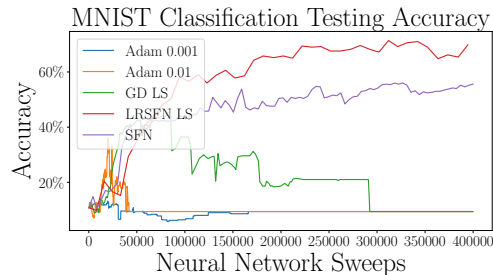


Figure 3. MNIST classification testing accuracy

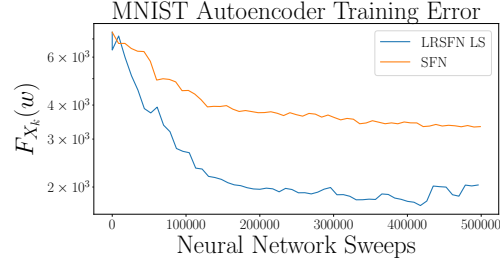


Figure 4. MNIST training error comparison SFN vs LRSFN

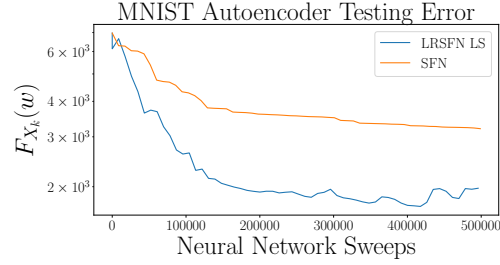


Figure 5. MNIST testing error comparison SFN vs LRSFN

First we present a head-to-head comparison of LRSFN and SFN for the same Hessian and gradient batches sizes, $N_{X_k} = N_{S_k} = 1000$. Figures 4 and 5 demonstrate that for the MNIST autoencoder training problem, LRSFN outperformed SFN. In what follows we have a general comparison of methods for MNIST and CIFAR10 autoencoder training problems. Guided by analysis, we advocate for using large gradient data batches for LRSFN, since the gradient sampling error shows up as a constant term in convergence rate bounds such as expression (12). We use $N_{X_k} = 10000$ for LRSFN and GD accordingly, and use line search for both. For Adam and SFN we take $N_{X_k} = 1000$, and for Adam we choose step lengths of $\alpha_k = 0.1, 0.01$. For both SFN and LRSFN we take the Hessian data batch size to be $N_{S_k} = 1000$.

For the MNIST dataset, Figures 6 and 7 show that LRSFN performed better both in terms of training and generalization error than any of the other methods. Both Adam with $\alpha_k = 0.1$ and GD with line search performed better than the SFN algorithm on this particular problem. Adam with $\alpha_k = 0.01$ was too slow to converge in the allotted number of neural network sweeps.

Similarly for the CIFAR10 dataset, Figures 8 and 9 show that LRSFN performs the best in both testing and training error, although in this case gradient descent with line search performs almost as well. SFN is not far behind, and both Adams variants do not perform well and tend to overfit. Note that LRSFN is implemented with a non-monotone line search: after five backtracking iterations have been performed, if no descent direction is found, LRSFN takes

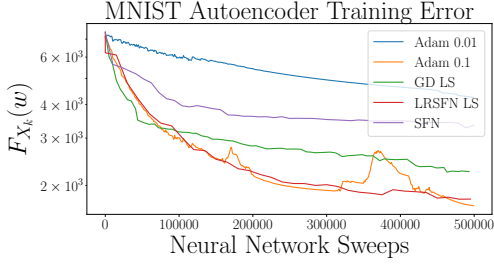


Figure 6. General comparison of training errors for MNIST autoencoder training

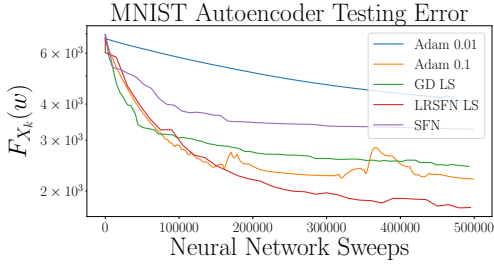


Figure 7. General comparison of testing errors for MNIST autoencoder training

the step anyway; this leads to spikes that can be seen in Figure 8.

As in other work, we observe the Hessian to be highly indefinite and have high rank at random initial guesses, but have numerical low rank after a few iterations (Alain et al., 2019; Ghorbani et al., 2019; Sagun et al., 2016). In the paper of Dauphin, numerical results showed that the magnitude of the largest negative eigenvalues decreased during the iterates of the SFN algorithm (Dauphin et al., 2014). We observe similar behavior for the MNIST autoencoder problem. In the MNIST problem the largest negative eigenvalue decreased by four orders of magnitude between the initial guess and the 70th iterate. In contrast Figure 12 shows that SFN is unable to escape the indefinite regions as well as LRSFN.

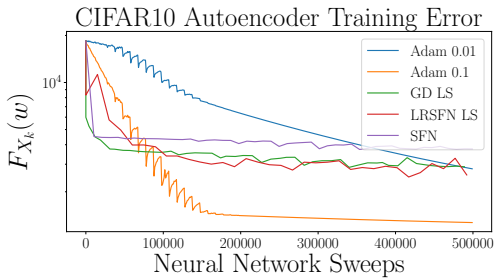


Figure 8. General comparison of training errors for CIFAR10 autoencoder training

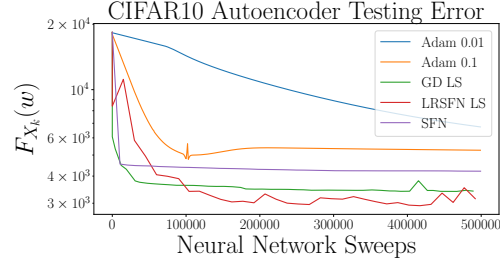


Figure 9. General comparison of testing errors for CIFAR10 autoencoder training

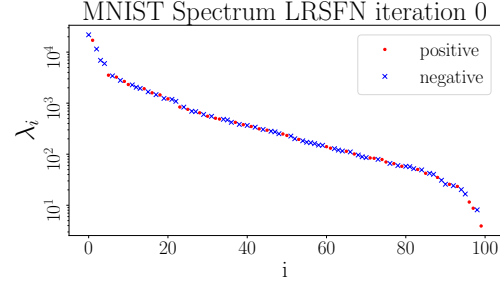


Figure 10. Spectrum of MNIST autoencoder training problem Hessian at initial guess

The effect of escaping negative definite regions can be seen even more for the CIFAR10 spectra in Figures 13 and 14. At the initial guess for CIFAR10 the Hessian is highly indefinite and at the 70th iterate of LRSFN at least the first 100 eigenvalues are positive. Figure 15 demonstrates again that SFN is unable to escape the indefinite regions as well as LRSFN.

In what follows we investigate the variance of the dominant 100 eigenvalues of the Hessian during training. We compute one spectrum with $N_{S_k} = 10,000$, and ten further sub-sampled Hessians with $N_{S_k} = 1,000$. In Figures 16 through 21 we use “full” to denote the 10,000 sample Hessian, and “sub i ” to denote the i^{th} 1,000 sample Hessian. The general trend in Figures 16 through 21 is that the

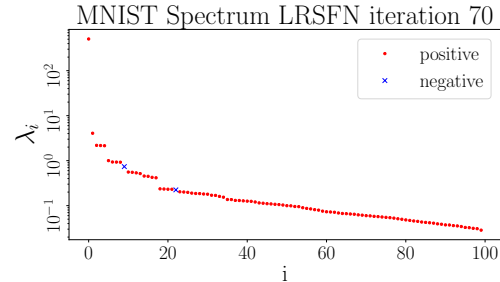


Figure 11. Spectrum of MNIST autoencoder training problem Hessian after 70 iterations of LRSFN

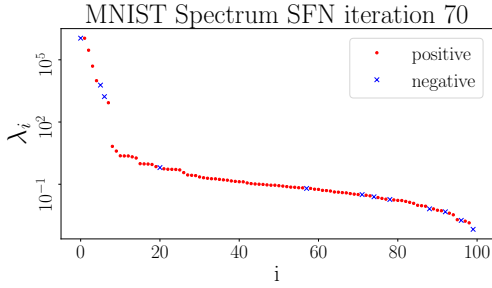


Figure 12. Spectrum of MNIST autoencoder training problem Hessian after 70 iterations of SFN

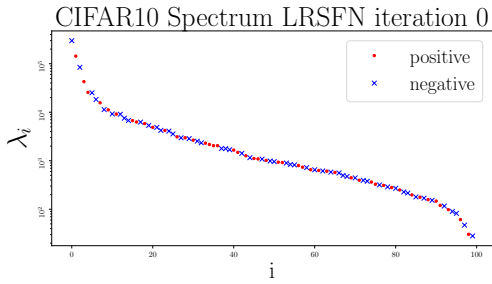


Figure 13. Spectrum of CIFAR10 autoencoder training problem Hessian at initial guess

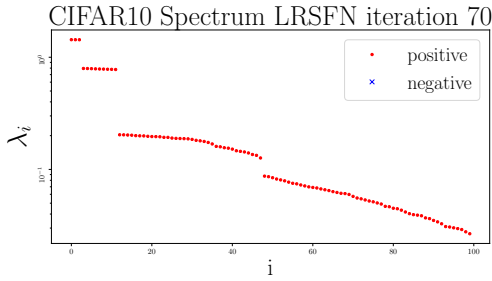


Figure 14. Spectrum of CIFAR10 autoencoder training problem Hessian after 70 iterations of LRSFN

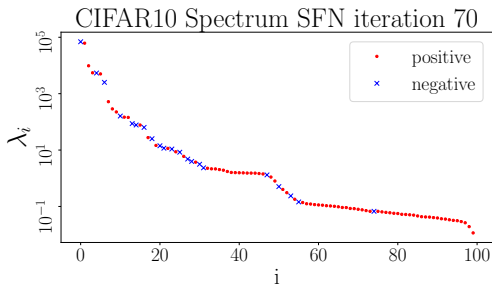


Figure 15. Spectrum of CIFAR10 autoencoder training problem Hessian after 70 iterations of SFN

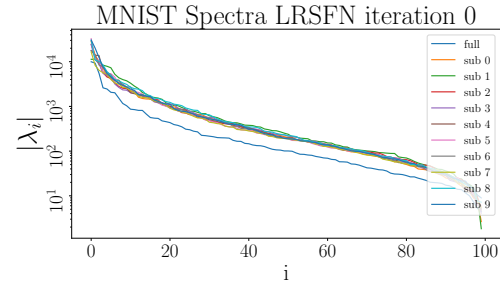


Figure 16. Subsampled Hessian spectra for MNIST at iteration 0

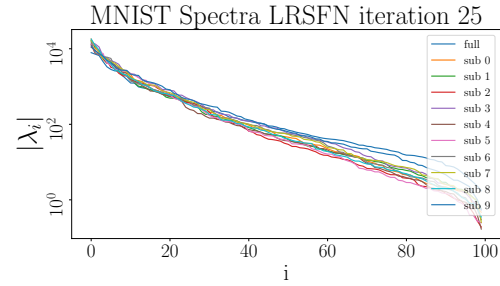


Figure 17. Subsampled Hessian spectra for MNIST at iteration 25

subsampled Hessians agree with the “full” Hessian for the dominant eigenvalues, but diverge for the trailing eigenvalues. This supports our claim that LRSFN is well suited for use with subsampled Hessians, because a low rank approximation of the subsampled Hessian is a good approximation of the dominant modes of the full Hessian.

For the CIFAR10 dataset we investigate the effect of Hessian batch size N_{S_k} on the convergence of the LRSFN algorithm. Figure 22 shows that similar convergence was observed from $N_{S_k} = 50$ all the way to 10,000. In this case not much was gained by using the full batch. Figure 23 demonstrates that significant computational economy can be had by Hessian subsampling. Second order methods do not require more work than first order methods per outer iteration; because the Hessian can be aggressively subsampled they only need be slightly more expensive per iteration.

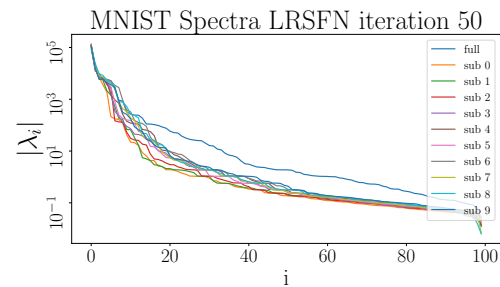


Figure 18. Subsampled Hessian spectra for MNIST at iteration 50

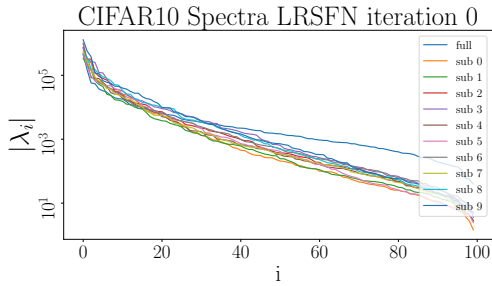


Figure 19. Subsampled Hessian spectra for CIFAR10 at iteration 0

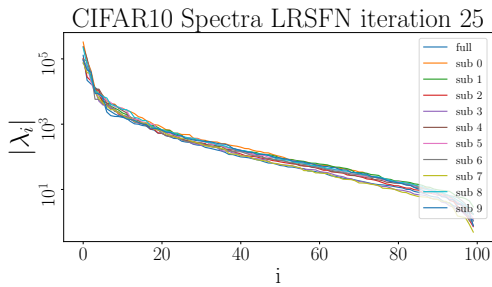


Figure 20. Subsampled Hessian spectra for CIFAR10 at iteration 25

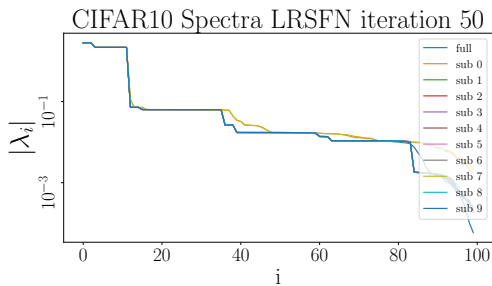


Figure 21. Subsampled Hessian spectra for CIFAR10 at iteration 50

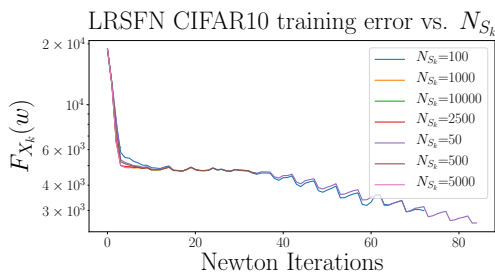


Figure 22. LRSFN training error vs Newton iteration for different Hessian batch sizes.

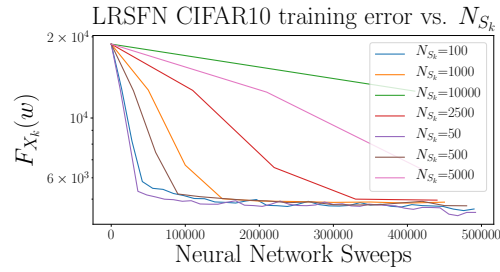


Figure 23. LRSFN training error vs neural network sweeps for different Hessian batch sizes.

Code used to generate these results can be found in the following repository (O’Leary-Roseberry, 2020).

6. Conclusion

In this paper we presented the low rank saddle free Newton (LRSFN) method. A randomized method is used to form a low rank approximation of the loss Hessian. The absolute value of the low rank approximation is used in conjunction with the Sherman-Morrison-Woodbury formula to solve the regularized Newton linear system.

The low rank approximation captures the dominant subspace of the Hessian better than the Lanczos method used in the SFN method (Dauphin et al., 2014). Resolving the dominant subspace of the Hessian allows iterates to escape indefinite regions with large negative eigenvalues faster. When subsampling is used to construct the Hessian, our results show that the dominant subspace of the full Hessian is well-approximated by the dominant subspace of subsampled Hessians, while the trailing subspace is less well-approximated. Thus low rank approximation, which captures the dominant subspace and ignores the trailing subspace, yields better generalization than Lanczos approximation, which attempts to approximate the entire spectrum at once. Moreover, the randomized low rank algorithm is inherently parallel, unlike Krylov based methods.

We prove a semi-stochastic convergence rate bound for the method, which shows that the LRSFN method can achieve fast convergence in expectation with respect to the Hessian batching.

We numerically test the LRSFN algorithm on two standard neural network benchmark problems, MNIST and CIFAR10. Numerical results show that the LRSFN algorithm outperforms the SFN algorithm as well as standard first order methods in both classification and autoencoder training problems. The LRSFN algorithm achieves faster convergence and better generalization error than the other methods.

References

- Alain, G., Roux, N. L., and Manzagol, P.-A. Negative eigenvalues of the Hessian in deep neural networks. *arXiv preprint arXiv:1902.02366*, 2019.
- Bertsekas, D. P. Nonlinear Programming. *Journal of the Operational Research Society*, 48(3):334–334, 1997.
- Bollapragada, R., Byrd, R. H., and Nocedal, J. Exact and inexact subsampled Newton methods for optimization. *IMA Journal of Numerical Analysis*, 39(2):545–578, 2018.
- Dauphin, Y. N., Pascanu, R., Gulcehre, C., Cho, K., Ganguli, S., and Bengio, Y. Identifying and attacking the saddle point problem in high-dimensional non-convex optimization. In *Advances in neural information processing systems*, pp. 2933–2941, 2014.
- Erdogdu, M. A. and Montanari, A. Convergence Rates of Sub-sampled Newton Methods. In Cortes, C., Lawrence, N. D., Lee, D. D., Sugiyama, M., and Garnett, R. (eds.), *Advances in Neural Information Processing Systems 28*, pp. 3052–3060. Curran Associates, Inc., 2015.
- Fernandes, D. SaddleFreeOptimizer. <https://github.com/dave-fernandes/SaddleFreeOptimizer/>, 2019.
- Ge, R., Huang, F., Jin, C., and Yuan, Y. Escaping from saddle points online stochastic gradient for tensor decomposition. In *Conference on Learning Theory*, pp. 797–842, 2015.
- Ghorbani, B., Krishnan, S., and Xiao, Y. An Investigation into Neural Net Optimization via Hessian Eigenvalue Density. *arXiv preprint arXiv:1901.10159*, 2019.
- Gill, P. E., Murray, W., and Wright, M. H. *Practical optimization*. Academic press, 1981.
- Halko, N., Martinsson, P.-G., and Tropp, J. A. Finding structure with randomness: Probabilistic algorithms for constructing approximate matrix decompositions. *SIAM review*, 53(2):217–288, 2011.
- Jin, C., Ge, R., Netrapalli, P., Kakade, S. M., and Jordan, M. I. How to escape saddle points efficiently. *arXiv preprint arXiv:1703.00887*, 2017.
- Krizhevsky, A., Nair, V., and Hinton, G. CIFAR-10 (Canadian Institute for Advanced Research). 2010. URL <http://www.cs.toronto.edu/~kriz/cifar.html>.
- LeCun, Y. and Cortes, C. MNIST handwritten digit database. 2010. URL <http://yann.lecun.com/exdb/mnist/>.
- Lee, J. D., Simchowitz, M., Jordan, M. I., and Recht, B. Gradient descent only converges to minimizers. In *Conference on learning theory*, pp. 1246–1257, 2016.
- Lee, J. D., Panageas, I., Piliouras, G., Simchowitz, M., Jordan, M. I., and Recht, B. First-order methods almost always avoid saddle points. *arXiv preprint arXiv:1710.07406*, 2017.
- Martinsson, P. G. and Tropp, J. Randomized Numerical Linear Algebra: Foundations & Algorithms. *arXiv preprint arXiv:2002.01387*, 2020.
- Murty, K. G. and Kabadi, S. N. Some NP-complete problems in quadratic and nonlinear programming. *Mathematical programming*, 39(2):117–129, 1987.
- O’Leary-Roseberry, T. hessianlearn. <https://github.com/tomoleary/hessianlearn>, 2020.
- O’Leary-Roseberry, T., Alger, N., and Ghattas, O. Inexact Newton methods for stochastic non-convex optimization with applications to neural network training. *arXiv preprint arXiv:1905.06738*, 2019.
- Roosta-Khorasani, F. and Mahoney, M. W. Sub-sampled Newton methods i: globally convergent algorithms. *arXiv preprint arXiv:1601.04737*, 2016a.
- Roosta-Khorasani, F. and Mahoney, M. W. Sub-sampled Newton methods ii: Local convergence rates. *arXiv preprint arXiv:1601.04738*, 2016b.
- Saad, Y. *Iterative methods for sparse linear systems*, volume 82. siam, 2003.
- Sagun, L., Bottou, L., and LeCun, Y. Eigenvalues of the hessian in deep learning: Singularity and beyond. *arXiv preprint arXiv:1611.07476*, 2016.
- Xu, P., Yang, J., Roosta-Khorasani, F., Ré, C., and Mahoney, M. W. Sub-sampled Newton Methods with Non-uniform Sampling. In Lee, D. D., Sugiyama, M., Luxburg, U. V., Guyon, I., and Garnett, R. (eds.), *Advances in Neural Information Processing Systems 29*, pp. 3000–3008. Curran Associates, Inc., 2016.